# Research on Designing the Regenerative Braking System Apply to Conventional Vehicle

***Duong Tuan Tung**, *Do Van Dung, Nguyen Truong Thinh***

*Ho Chi Minh City University of Technology and Education, No. 1 Vo Van Ngan, Thuduc, Ho Chi Minh, Vietnam*

*Received: December 18, 2018; Accepted: June 24, 2019*

**Abstract**

*This study will calculate, design, and fabricate the inertial energy recovery model of the vehicle during braking or deceleration. This energy recovery unit is applied to conventional vehicles, including a double planetary gear set which is installed parallelly with the propeller shaft and a generator which is coaxial with the flywheel in order to convert the mechanical energy into electricity to recharge for the battery. The simulations and experimental models are built and controlled in the FTP75; NEDC; EUDC and ECR15 driving cycles. When the vehicle's deceleration occurs, the energy recovery process will start. The control method for regenerative energy optimization is used for both simulation and experimental models. Experimental results show that the recovered energy is in the range of 22% to 38% of the inertial energy of the vehicle during the deceleration process. This energy is converted into electricity which will be used for additional loads on the vehicle.*

Keywords: Regenerative Braking System (RBS), Kinetic Energy Recovery Storage (KERS), Planetary Gear Unit, Conventional Powertrain System, Braking Force Distribution.

## 1. Introduction

Regenerative braking system (RBS) is designed for recovering and reusing the inertia energy of the vehicle during braking or deceleration. It contributes to the reduction in fuel consumption and the increase in the lifetime of the braking mechanism [1-3]. One of the most important factors affecting performance is the method of recovery, storage, and re-usage of vehicle inertia energy. Currently, the regenerative braking energy storage technologies are divided into different types such as flywheels, supercapacitors, batteries, the hydraulic energy storage or combination of flywheel and electric storage devices [4-6].

The electric energy storage system needs to use batteries and supercapacitors with large capacity, high voltage inverter. It's applied for electric or hybrid electric vehicles with high cost [7]. The hydraulic storage system is a complex structure and effective only on the heavy-duty truck. On the other hand, a flywheel is low-cost and highly effective, especially when it is combined with other with devices such as supercapacitors or batteries will be good for conventional vehicle [8]. In this study, a kinetic energy recovery storage assembly will be calculated and designed with the aim to recapture the vehicle inertia energy while braking or deceleration with the experimental model in Fig.1. The model is a combination of a conventional flywheel and generator which are used to convert mechanical energy into electric energy.

* Corresponding author: Tel.: (+84) 914.805.623
Email: tungdt@hcmute.edu.vn

General description of the system: The drivetrain of the conventional vehicle is connected to the regenerative braking energy recovery assembly via the double planetary gear set which enables the transmission inertia force of vehicle to transmit directly to the flywheel when the vehicle brakes or decelerates. Flywheel and generator are connected coaxially to convert mechanical energy into electricity.

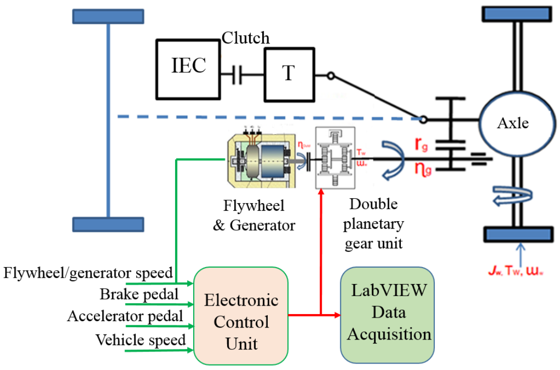


**Fig 1.** The block diagram of the experimental model

## 2. Calculation and design of energy recovery assembly.

### *2.1. Mathematically model*

Based on the general description, the inertia energy recovery assembly consists of a chain; a double planetary gear unit; a flywheel which is connected to the generator coaxially; a control system and a data acquisition system. Calculation and designing parameters such as chain ratio; the planetary gear and flywheel dimensions are determined based on Toyota Hiace vehicle.

Assuming that the vehicle is moving down a slope with the slope angle is θ, the engine works at idle speed (no propulsive force at the drive wheels). At that time, the forces acting on the vehicle are shown in Fig.2.

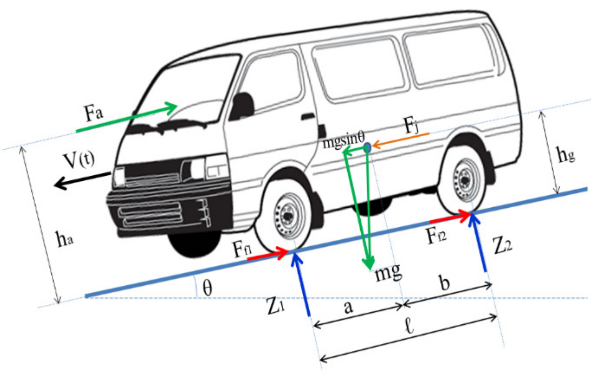


**Fig. 2.** The free-body diagram of the forces acting on the vehicle

When the vehicle starts decelerating, the driving force of the vehicle will be the inertia force at that moment. Along with that, there are aerodynamic drag force, rolling resistance force and slope resistance force, etc. which are acting in an opposite direction. Therefore, the drive wheel moment (rear-wheel drive) is determined:

$$M_b = M_j + M_\theta - M_f - M_a \tag{1}$$

Where $M_b$ is drive wheel moment [N.m];

$M_j$ is vehicle inertia moment;

$M_\theta$ is slope resistance moment

$$M_\theta = m.g.\sin\theta.r_b \tag{2}$$

$M_f$ is rolling resistance moment

$$M_f = f.m.g.\cos\theta.r_b \tag{3}$$

$M_a$ is aerodynamic drag moment

$$M_a = 0.5.\rho.A.C_D\left(V + V_{wind}\right)^2.r_b \tag{4}$$

Here, $r_b$ is the effective radius of the tires [m]; $V$ is the velocity of vehicle [m/s] and $V_{wind}$ is the wind velocity [m/s].

$M_j$ is inertia moment of the vehicle including inertial moment of linear motion and inertial moment of rotational components in powertrain system such as engine, clutch, transmission, propeller shaft and drive wheels [9].

$$M_j = F_j.r_b = r_b.m.\frac{dv}{dt}.\delta_i \tag{5}$$

$$\delta_i = 1 + \frac{j}{m.r_b^2}\left(I_e.i_t^2.\eta_t + \sum I_n.i_n^2.\eta_n + \sum I_b\right) = 1 + \frac{I}{m.r_b^2} \tag{6}$$

Where $I_n$ is inertia moment of part n in powertrain system; $I_b$ is inertia moment of drive wheels [kg.m$^2$]; $I_t$ is ratio of powertrain system; $I_n$ is ratio of part n in powertrain to drive wheel; $\eta_t$ is efficiency of powertrain system; $\eta_n$ is efficiency of rotational part n to drive wheel; $I_e$ is inertia moment of rotational parts in the engine. $I_e$ is determined by equation [10], [11].

$$I_e = I_{cgi} + I_{fw} = (m_c + m_{cr})R_c^2.n_{cyl} + I_{fw} \tag{7}$$

In the above formula, $I_{cgi}$ is the inertia moment of crankshaft and its attached parts [kg.m$^2$]; $I_{fw}$ is the inertia of flywheel; $m_c$ is the mass of crankshaft [kg.m$^2$]; $m_{cr}$ is the mass of the big end of connecting rod [kg]; $n_{cyl}$ is the number of cylinders.

Inertia moment of transmission $I_h$ is determined by equation (8) [11], [12].

$$I_h = I_I + I_{II}.i_a^{-2} + \sum_{k=1}^{m} I_{zk}.i_k^{-2} + I_l.i_l^{-2} \tag{8}$$

Where $I_I$ is inertia moment of input shaft; $I_{II}$ is inertia moment of intermediate shaft; $i_a$ is ratio of gears always meshed; $I_{zk}$ is inertia moment of idle gear on output shaft; $i_k$ is ratio of transmission at gear k engaged; m is number of idle gears on output shaft; $I_l$ is inertia moment of reverse gears; $i_l$ is ratio of reverse gear.

After clarifying all the parameters to determine the inertia moment of vehicle, the torque acting on the half shaft of the drive axle can be calculated by equation (9).

$$M_b = r_b(m.\frac{dv}{dt}.\delta_i - f.m.g.\cos\theta - 0.5\rho.A.C_D\left(V + V_{wind}\right)^2 + m.g.\sin\theta) \tag{9}$$

The torque of the generator shaft will be:

$$M_{mp} = i_{rbs}.r_b(m.\frac{dv}{dt}\delta_i - f.m.g.\cos\theta - 0.5\rho.A.C_D.V_{(t)}^2 + m.g\sin\theta) \tag{10}$$

$$M_{mp} - M_{ton\_hao} = J.\frac{d\omega_{mp}}{dt} \tag{11}$$

$$\omega_{mp} = \frac{1}{J}(\int M_{mp} - M_{ton\_hao})\,dt \tag{12}$$

In this case, $J = J_f + J_{roto\_ge}$ is the rotational inertia of flywheel and generator rotor.

The energy balance equation of the generator is defined as follow:

$$P_{truc\_mp} - P_{ton\_hao} = P_{ra} \tag{13}$$

$$M_{mp} - \frac{P_{ton\_hao}}{\omega_{mp}} = 3E_s.I_s.\cos f\varphi \tag{14}$$

The equation expressing the relationship between generator output and vehicle deceleration during braking or deceleration is defined as equation (15).

$$[i_{rbs}.r_b(m.\frac{dv}{dt}\delta_i - f.m.g.\cos\theta - 0.5\rho.A.C_D.V_{(t)}{}^2 + m.g.\sin\theta)]$$

$$-\frac{P_{ton\_hao}}{\omega_{mp}} = 3E_s.I_s.\cos\varphi \tag{15}$$

Where: $E_s = K_M.I_s.\omega_{mp}$

$i_{rbs}$ is the ratio of recovery energy unit; $r_b$ is wheel radius; $\delta_i$: rotational inertia coefficient; $P_{ton\_hao}$ is the loss power including the mechanical loss and electrical loss; $E_s$ and $I_s$ are voltage and current of the generator.

### 2.2. Simulation model

To calculate the energy recovery efficiency, FTP-75, NEDC, EUDC and ECE R15 driving cycles are used for simulating.

Simulation process description: At the beginning of simulation, the standard driving cycle is uploaded onto the system. The engine output power will be then controlled by the controller based on the acceleration graph of the standard driving cycle. When the deceleration signal is recorded, the control system starts activating the energy recovery unit and the hydraulic braking system operates to ensure that the actual speed of the vehicle will match the vehicle speed in the standard driving cycle. In order to control the torque changing of the vehicle, a PID controller is set up to control the transmission ratio. During the recovery energy unit operation, the generator speed is altered in the range with an optimum performance by the CVT controller.

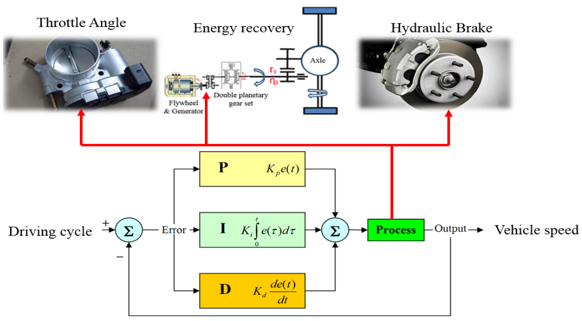


**Fig. 3.** Block diagram of the simulation

**Table 1.** Simulation vehicle parameters (Toyota Hiace-2003)

| Parameters | Value |
|---|---|
| Wheel base (mm) | 2570 |
| Width (mm) | 1430 |
| Ground clearance (mm) | 182 |
| Weight (kg) | 1905 |
| Maximum power (kW/rpm) | 74/5400 |
| Maximum Torque (Nm/rpm) | 165/2600 |
| Ratio at 1st gear | 4.452 |
| Ratio at 2nd gear | 2.619 |
| Ratio at 3rd gear | 1.517 |
| Ratio at 4th gear | 1.000 |
| Ratio at 5th gear | 0.854 |
| Reverse ratio | 4.472 |
| Final drive ratio | 4.3 |
| Frontal area ($m^2$) | 2.325 |
| Wheel radius (m) | 0.33 |

**Table 2.** Rotational inertia coefficient ($\delta_i$)

| Gear | 1 | 2 | 3 | 4 | 5 |
|---|---|---|---|---|---|
| Ratio | $i_{h1}$= 4.452 | $i_{h2}$= 2.619 | $i_{h3}$= 1.517 | $i_{h4}$= 1 | $i_{h5}$= 0.895 |
| $\delta_i$ | 1.355 | 1.2115 | 1.0975 | 1.065 | 1.066 |

PID transfer function is determining as equation:

$$G_{PID(z)} = K_p + K_I.T_s\frac{1}{Z-1} + K_D.\frac{1}{T_s}.\frac{z-1}{z} \tag{16}$$

Where $K_p$=0.41014; $K_I$=0.11687; $K_D$=0; $T_S$=0.01.

Accelerator transfer function:

$$G_{(z)} = \frac{0.054}{z-0.946} \tag{17}$$

$$G_{h(z)} = G_{PID(z)}.\ G_{(z)} \tag{18}$$

$$G_{PID(z)} = \frac{K_P.(z-1).z.T_s + K_I.T_s^2.z + K_D.(z-1)^2}{T_s.z.(z-1)}$$

$$G_{PID(z)} = \frac{z^2.(K_P.T_s + K_D) + z.(K_P T_s - K_I.T_s^2 + 2.K_D) + K_D}{T_s.z.(z-1)}$$

$$G_{PID(z)} = \frac{41014.10^{-3}.z - 4089713.10^{-3}}{0.01z - 0.01}$$

$$G_{h(z)} = \frac{2.214756.10^{-4}.z - 2.20844502.10^{-4}}{(z-0.946)(0.01z-0.01)}$$

Transfer function of RBS system:

$$G_{k(z)} = \frac{Y_{(z)}}{R_{(z)}} = \frac{G_{PID(z)}.G_{(z)}}{1 + G_{PID(z)}.G_{(z)}} \tag{19}$$

$$G_{k(z)} = \frac{G_{h(z)}}{1 + G_{h(z)}} \tag{20}$$

$$G_{k(z)} = \frac{2.214756.10^{-4}.z - 2.20844502.10^{-4}}{0.01z^2 - 0.019z + 9.2392.10^{-3}}$$

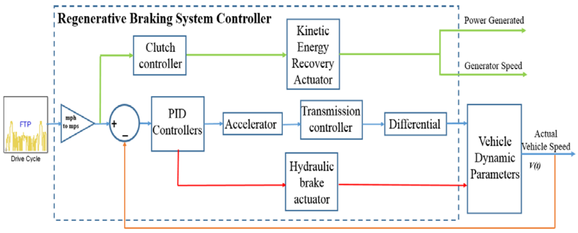


**Fig. 4.** Simulation model in MATLAB Simulink

In the simulation, the control method based on the optimal energy recovered. The control signals are shown in **Fig. 5.**

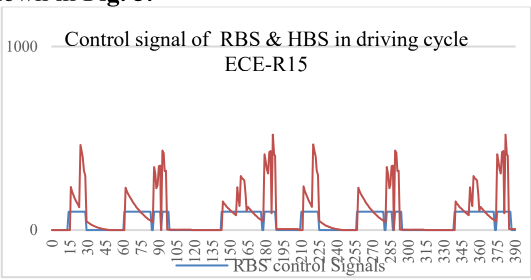


**Fig. 5.** Output control of the braking controller

Based on the simulation results in MATLAB Simulink, by using SolidWorks software a 3D model was built on Fig.6a. Fig.6b is the combination of SolidWorks and ADAMS/VIEW for dynamic simulation and stability testing.

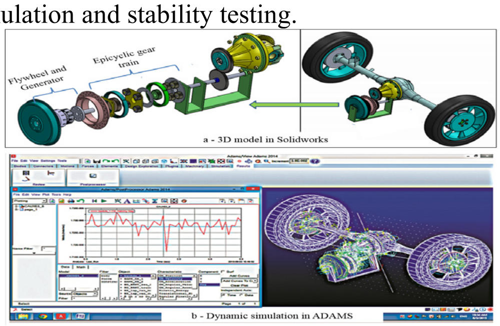


**Fig. 6.** Experimental model in SolidWorks and ADAMS

### *2.3. Experimental model*

General description of the experimental model: the vehicle speed signal from the actual model of the vehicle is controlled based on the frequency converter to control the electric motor. Electric motors will drive the axle to rotate the drive wheel. There are load generating devices and torque sensors which are mounted on the half shaft to determine the torque applied to the drive wheels. Along with that, the controller also controls the traction of the motor so that the velocity of the vehicle in the experiment model is equal to the standard driving cycle.

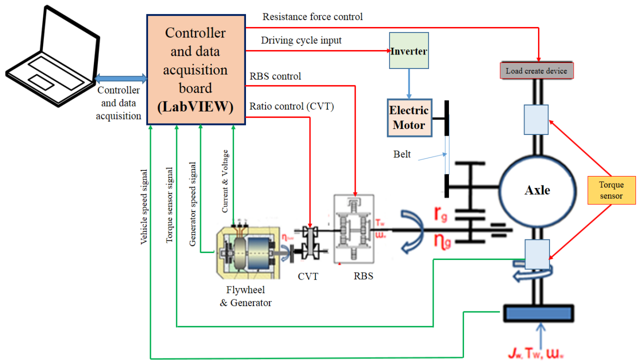


**Fig.7.** Experimental model diagram

The driving axle is connected to the RBS unit via a double planetary gear which allows the inertia to be delivered to the flywheel during braking or deceleration. The flywheel and generator are coaxial in order to convert mechanical energy into electricity. The PID controller keeps the vehicle speed equal to driving cycles. Load-creating device and torque sensor have been used to measure the braking force at the drive wheels. During the decelerating process, the controller will activate the energy recovery system; change ratio of CVT and control the current and voltage generated by the generator.

In order to experimentally evaluate the efficiency of the recovery system, experiments will be conducted with full driving cycles. Specifications of the components in the experimental model are shown in Table 3

**Table 3.** Parameters of the experimental model.

| Name | Parameters |
|---|---|
| Motor | Toshiba 3 phases -220V ; 7.5kW |
| Inverter | Toshiba VF-FS1 ; 3 phases -220V ; 7.5kW |
| Magnetic braking | VSED ; 80V- 4.7A ; 1800rpm |
| Torque sensor | Burster Torque sensor 85646 ; 0-500Nm ; 2.34mV/Nm |
| Controller and data acquisition | Card NI USB6008<br>Aduino-uno<br>LabVIEW 2014<br>Magnetic sensor are used to measure vehicle speed and generator speed |
| RBS Ratio | 0.1< i<0.6 |
| Generator | 2HP |
| Load device | $I_{max}$ 50A ; U 20V |

The experiment is carried out with 4 different driving cycles: FTP-75, NEDC, EUDC, and ECE R15. Each cycle is installed to the inverter driving the motor through the PID controller. During vehicle speed sensor operation, the feedback signal allows the PID controller to continuously control the actual speed of the vehicle match with the standard speed of the driving cycle. In addition, the magnetic brakes on the wheel are activated to slow down the vehicle speed. Whenever a deceleration signal appears, the controller activates the energy recovery system through a double planetary gear set, which spins the flywheel and generator. The energy recovery process starts. The energy generated by the generator will be supplied through an adjustable load. During the working process, the data acquisition system through LabVIEW software will always record the values such as vehicle velocity, generator speed, voltage and current through the load.

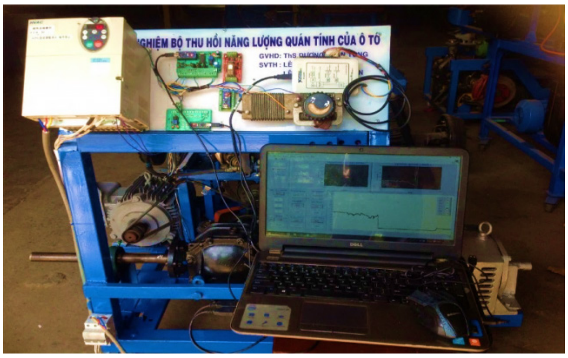

**Fig. 8.** Data acquisition using LabVIEW

## 3. Result analysis and discussion

### *3.1. Simulation result:*

Based on the simulation results of the full driving cycle, the energy recovered is calculated. From the power curve data, the energy generated can be determined by equation (21) [13], [14].

$$E = \int_{t_0}^{t_n} P_{(t)} dt \qquad (21)$$

If the obtained power is a line which is parallel to the time axis, the energy obtained is calculated as the equation below:

$$E = P.\Delta t = P(t_n - t_0) \qquad (22)$$

The total energy recovered by FTP-75 driving cycle is: $\sum E = 18038.41(kJ)$ with full driving cycle duration 3748(s) and active duration of RBS 1145(s); The NEDC is: $\sum E = 2478.09(kJ)$ with full driving cycle duration 180(s) and active duration of RBS 238 (s); The EUDC driving cycle is: $\sum E = 1745.52\ (kJ)$ with full driving cycle duration 400(s) and active duration of RBS 94 (s); The ECE R15 driving cycle is: $\sum E = 209.022(kJ)$ with full driving cycle duration 195(s) and active duration of RBS 36 (s)

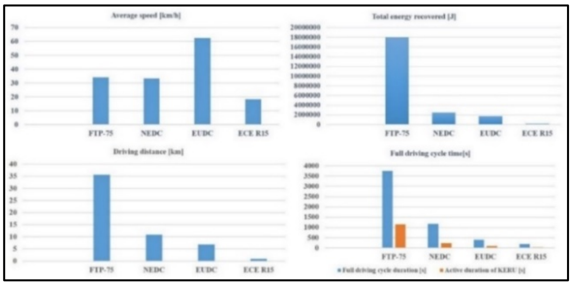


**Fig. 9.** Chart of comparing simulation results between cycles

### *3.2. Experimental result*

According to the graph built based on the data of the experimental results, the energy recovery time is less than the simulation result. Because of the electrical latency phenomenon, when the system detects the deceleration of the vehicle through the speed sensor, the controller immediately activates the RBS. However, mechanical adaptation can slow the speed of the energy recovering process increment. In addition, deceleration stages often occur shortly, just about 2 to 3 seconds and then return to the acceleration mode. In these situations, the energy recovering system is often disabled during the experiment.

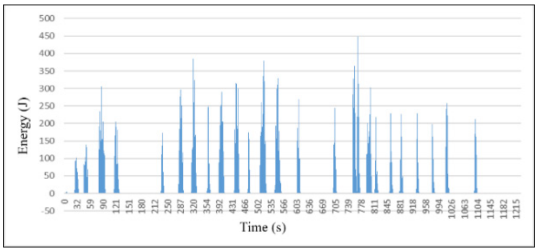


**Fig. 10.** Energy recovered on the FTP 75 driving cycle

The total energy recovered by FTP-75 driving cycle $\sum E = 5050.75(kJ)$

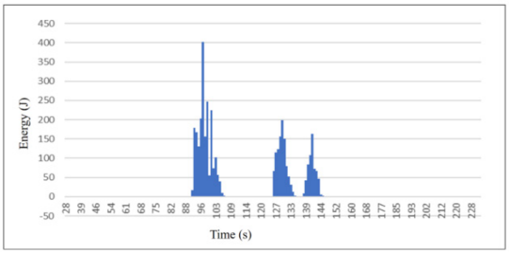


**Fig. 11.** Energy recovered on the ECE R15 driving cycle

**Table 4.** The results of energy recovered in driving cycles.

| Driving cycle | | FTP-75 | NEDC | EUDC | ECE R15 |
|---|---|---|---|---|---|
| Driving distance [km] | | 35.54 | 109.314 | 69.549 | 0.9941 |
| Full driving cycle duration [s] | | 3748 | 1180 | 400 | 195 |
| Active duration of RBS [s] | | 1145 | 238 | 94 | 36 |
| Percentage of active duration (%) | | 30.5% | 20.2% | 23.5% | 18.5% |
| Average speed [km/h] | | 34.1 | 33.35 | 62,59 | 18.35 |
| Total energy recovered [kJ] | Simulation | 18038.41 | 2478.09 | 1745.52 | 209.02 |
| | Experiment | 5050.75 | 792.99 | 663.29 | 45.98 |
| Efficiency | | 0.28 | 0.32 | 0.38 | 0.22 |

The total energy recovered by ECE R15 driving cycle: $\sum E = 459.84(kJ)$

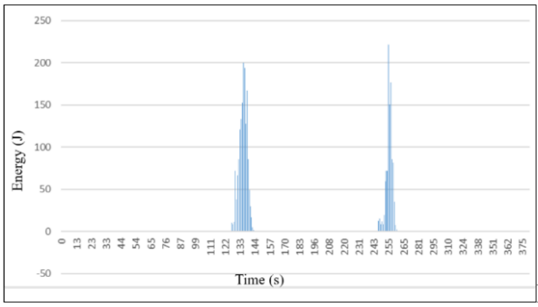


**Fig. 12.** Energy recovered on the EUDC driving cycle

The total energy recovered by EUDC driving cycle: $\sum E = 663.29(kJ)$

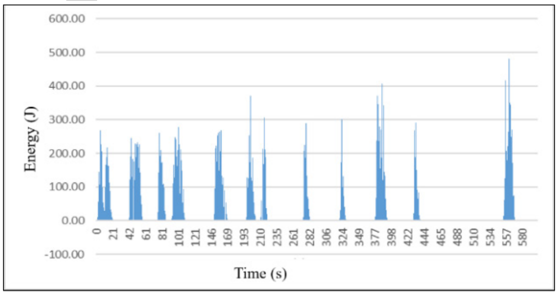


**Fig. 13.** Energy recovered on the NEDC driving cycle

The total energy recovered by NEDC driving cycle: $\sum E = 792.99(kJ)$

**Discussion**

According to the experimental results, the recovered energy can be various from 28% to 38% of the energy according to the simulation results. Energy recovery is also depending on the driving cycle. The more deceleration time is activated in the driving cycle; the more energy is recovered.

With the FTP75 driving cycle, the energy recovery rate can reach up to 30.5% although the energy recovery efficiency is not so high because the vehicle speed at the beginning of the deceleration process is low. Besides, the active duration of RBS for each energy recovery is not that long due to the city driving conditions.

With the EUDC driving cycle, although the activation period of RBS is only 23.5% in total, the energy recovery efficiency can reach up to 38% thanks to the vehicle speed at the beginning of the deceleration process is higher than FTP75.

The braking force distribution also affects significantly the amount of energy recovered. There are three control methods for the regenerative braking force distribution such as optimizing braking force; maximizing recovered energy and collaborating to ensure the stability while braking. In this study, the braking force from the energy recovery system is controlled by the balance between the regenerative braking force and mechanical braking to keep the vehicle stable.

## 4. Conclusion

This paper presented the design and calculated parameters of the regenerative braking system based on conventional vehicle powertrain. The experimental results demonstrate the energy recovery efficiency which can reach up to 38% depends on the initial velocity of the braking process. The higher the velocity of the vehicle at the beginning of braking process is; the larger the energy recovery generated by regenerative braking assembly will be. These results will be the fundament for optimizing the structural calculation of mechanical system along with the fuel consumption of the vehicles equipped with the regenerative braking energy recover assembly. In order to improve the efficiency even more, there will be further studies on reducing mechanical loss by using magnet bearing and placing the flywheel on vacuum chamber. Furthermore, the control algorithms and methods should also be improved.

**Acknowledgements**

The authors would like to thank the president of HCMUTE, supervisors, Automotive Mechatronic Lab, Automotive Testing Lab at Faculty of Vehicle and Energy Engineering for supporting us in this research.

**References.**

[1]. Farhan Khan, Shivam Kumar, Dr.Ashish Mathew, Int. J. of Innovative Research in science and Engineering, Vol.No.2, Issue 04, April 2016.

[2]. C. M. Jefferson and M. Ackerman; Int. J. of Energy Conversion and Management, vol. 37, pp. 1481-1491, 1996.

[3]. S. J. Clegg; A Review of Regenerative Brake System.Transport Studies, Working Paper 471, University of Leeds, UK, 1996

[4]. Mayuresh Thombre; Prajyot Borkar, Mangirish Bhobe; Int. J. of Mechanical, Aerospace, Industrial, Mechatronic and Manufacturing Engineering Vol: 8, No: 4, 2014

[5]. Loi Wei Cheong; Regenerative Braking System (RBS): Energy Measurement, University Technical Malaysia Melaka, Malaysia 2012

[6]. Fabian Perktold; Research on a regenerative braking system for a golf cart, University of Applied Sciences Upper Austria, Australia, 2016

[7]. Radhika Kapoor, C. Mallika Parveen, Member, IAENG, Comparative Study on Various KERS, paper presented at the World Congress on Engineering, London, U.K., 2013.

[8]. C. Brockbank and W. Body; Flywheel based mechanical hybrid system; simulation of the fuel consumption benefits of various transmission arrangements and control strategies; paper presented at the ASME International Design Engineering Technical Conferences & Computers and Information in Engineering Conference (IDETC/CIE '10), Montreal, Canada, 2010

[9]. Rajesh Rajamani; Vehicle Dynamics and Control (Springer Science+Business Media, LLC, 233 Spring Street, New York, NY 10013, USA) Page 98-101, 2012

[10]. Raffaele Di Martino; Modelling and Simulation of the Dynamic Behaviour of the Automobile, PhD thesis in Mechanical Engineering, University of Salerno, Italy, 2005.

[11]. Vu Thanh Trung, Nguyen Dinh Tuan, Nguyen Hoang Vu; Determination of rotating mass factor to simulating longitudinal motion dynamics of the Hyundai Starex vehicle; National conference on Mechanical Science and Technology, HCM city 2015.

[12]. Alberto A. Boretti; Int. J. Vehicle Design, Vol. 55, No. 1, 2011

[13]. Tai-Ran Hsu; On a Flywheel-Based Regenerative Braking System for Regenerative Energy Recovery, paper presented at the Green Energy and systems Conference, USA, 2013.

[14]. U. Diego Ayala, Martinez-Gonzalez, P., McGlashan, N., Pullen, K.R.; Int. J. of automobile Engineering, vol. 222, 2008.